Multiscale Simulation of Plasticity in bcc Metals

Daniel Weygand,[1] Matous Mrovec,[2] Thomas Hochrainer,[3] and Peter Gumbsch[1,2]

[1]Institute for Applied Materials, Karlsruhe Institute of Technology (KIT), 76131 Karlsruhe, Germany; email: peter.gumbsch@kit.edu

[2]Fraunhofer IWM, 79108 Freiburg, Germany

[3]Bremen Institute of Mechanical Engineering, University of Bremen, 28359 Bremen, Germany

Annu. Rev. Mater. Res. 2015. 45:369–90

First published online as a Review in Advance on February 11, 2015

The *Annual Review of Materials Research* is online at matsci.annualreviews.org

This article's doi: 10.1146/annurev-matsci-070214-020852

Keywords

dislocation, plastic deformation, atomistic modeling, dislocation dynamics, continuum theory, single crystal

Abstract

Significant progress in our understanding of plasticity in body-centered cubic (bcc) metals during the last decade has enabled rigorous multiscale modeling based on quantitative physical principles. Significant advances have been made at the atomistic level in the understanding of dislocation core structures and energetics associated with dislocation glide by using high-fidelity models originating from quantum mechanical principles. These simulations revealed important details about the influence of non-Schmid (nonglide) stresses on the mobility of screw dislocations in bcc metals that could be implemented to mesoscopic discrete dislocation simulations with atomistically informed dislocation mobility laws. First applications of dislocation dynamics simulations to studies of plasticity in small-scale bcc single crystals have been performed. Dislocation dynamics simulations inspired the development of continuum models based on advanced 3D dislocation density measures with evolution equations that naturally track dislocation motion. These advances open new opportunities and perspectives for future quantitative and materials-specific multiscale simulation methods to describe plastic deformation in bcc metals and their alloys.

INTRODUCTION

The first systematic investigations of the mechanical behavior of body-centered cubic (bcc) metals (1) revealed that their plasticity is fundamentally different from that of hexagonal and face-centered cubic (fcc) metals. Even though plastic slip in bcc metals was observed in the expected close-packed ⟨111⟩ directions, the slip traces did not coincide with a single crystallographic plane and varied with the orientation and sense of the applied stress (2). These findings were a clear violation of the Schmid law (3), which states that plastic flow is initiated when the resolved shear stress on the most stressed slip system reaches a critical value, the critical resolved shear stress (CRSS), and that this critical stress is not affected by any other component of the applied stress tensor (4). A number of deformation experiments (2) have shown that various bcc single crystals exhibit non-Schmid behavior such as tension-compression asymmetry, twinning-antitwinning asymmetry, and dominant slip on crystallographic planes with low Schmid factors at low temperatures (5, 6).

Some of the observed effects can be related to symmetry properties of the bcc crystal structure (7). However, to explain all the unusual phenomena, it is necessary to examine the intrinsic properties of dislocations as the carriers of plastic slip. Sir Peter Hirsch first proposed in 1960 that the peculiar plastic properties of bcc metals have their origin in a nonplanar spreading of the screw dislocation cores (P.B. Hirsch, oral contribution). Such a nonplanar core structure implies large Peierls stresses and makes the screw dislocations difficult to move. This hypothesis was supported by many transmission electron microscopy (TEM) observations (2, 8) that detected postdeformation dislocation microstructures dominated by long and mostly straight or jogged screw dislocations. Additional validation was then provided by atomistic simulations (9) that unequivocally confirmed the nonplanar character of screw dislocation cores in bcc metals.

The crucial role of screw dislocations and their cores in understanding the macroscopic plasticity of bcc metals has been a subject of several reviews (7, 10–12). Apart from explaining non-Schmid behavior, the core effects are also responsible for the pronounced temperature dependence of the flow stress because dislocation motion at low temperatures proceeds via the thermally activated nucleation and propagation of kink pairs on otherwise straight screw dislocations (13, 14). Such studies of individual dislocations, although important, represent only a first step in understanding and describing the macroscopic plasticity of bcc metals at finite temperatures. To link experimental results to the underlying nanoscale mechanisms, it is necessary to employ additional phenomenological models and theories that utilize only the essential properties of dislocations instead of covering all atomistic details. This approach enables one to capture timescales and length scales relevant for the description of macroscopic materials behavior.

In recent years, newly developed discrete dislocation dynamics (DDD) models (15) have provided a mesoscopic description of dislocation ensembles based on single-dislocation mobilities. These models require, as input, mobility laws for different dislocation segments and dislocation characters as a function of stress and temperature. Provided that these mobility laws are based on correct nanoscale dislocation behavior, DDD simulations can capture the interactions of multiple dislocations by their elastic fields and by dislocation reactions and quantitatively follow the evolution of dislocation microstructure during plastic deformation. Furthermore, a systematic coarse graining of discrete dislocation ensembles into continuum dislocation densities and dislocation fluxes then leads to the continuum mechanical formulation of plastic strain.

Such a multiscale modeling framework holds the promise not just of assessing the generic features of plastic deformation in bcc metals but also of making materials-specific modeling possible. In this case, complex phenomena such as the temperature dependence of plasticity, hardening, and the influences of crystal defects or alloying elements should in principle become accessible.

There have been growing efforts to pursue information transfer between the different levels of abstraction: from the atomistic investigation of dislocations to mobility laws for DDD, and from dislocation microstructure to continuum formulations of crystal plasticity describing the plastic deformation of bcc metals as a consequence of dislocation flow. This review aims to provide an overview of these efforts—to highlight the achievements but also to identify existing limitations and areas that still need to be developed. For simplicity, we focus here on continuous unidirectional deformation at low and intermediate temperatures and at typical loading conditions and strain rates, thereby mostly excluding high-temperature deformation, creep, fatigue, irradiation damage, fracture, and shock loading.

CORE EFFECTS AND ATOMISTIC PROPERTIES OF DISLOCATIONS

The properties of individual dislocations can be understood only when the atomic structure of their cores is properly taken into account. Detailed insights into the dislocation behavior at the atomic level can be obtained from atomistic simulations. Dislocation cores in bcc metals have been investigated from the onset of atomistic modeling, first using rudimentary classical interatomic potentials but gradually employing more complex and accurate descriptions of interatomic interactions (for recent reviews, see References 11, 12, and 16). Advancements in atomistic models, modeling methodologies, and computer performance during the last two decades have shifted the main focus from analyses of the generic behavior for the whole class of bcc materials to materials-specific issues related to chemical differences, environmental effects (e.g., external stress, interactions with other defects), and quantitative descriptions of dislocation motion.

The key prerequisite for a quantitative description of materials-specific behavior is a reliable description of interatomic interactions. The chemical bonding in bcc transition metals is characterized by strong, unsaturated, directional, covalent bonds originating from the interactions between valence *d*-electrons (17) and is further complicated by magnetic effects in case of bcc Fe. At present, the most reliable class of methods able to capture the subtleties of chemical bonding consists of first-principles methods based on density functional theory (DFT). Despite the fact that DFT calculations are still limited to system sizes not exceeding a few hundred atoms, such calculations have been extensively applied in simulations of $1/2\langle 111\rangle$ screw dislocations in bcc transition metals, helping to resolve several open questions regarding their behavior (18–28). The last decade has also seen an extensive development and application of advanced semiempirical schemes such as bond order potentials (BOPs) (29–32) and potentials based on first-principles generalized pseudopotential theory (GPT) (16, 33, 34). These schemes are derived by rigorous approximations to the electronic structure methods, so they correctly reflect the physics of bonding but can be applied to significantly larger atomic ensembles than can DFT calculations. In addition, they provide much larger flexibility in the choice of boundary conditions, which is often crucial for obtaining meaningful results in simulations of defects.

Core Structure and Energy

Most atomistic studies in the last few years continued to focus on the properties of the $1/2\langle 111\rangle$ screw dislocation. The nonplanar core structure of this screw dislocation is responsible for the unconventional aspects of plastic deformation such as unusually strong orientation and temperature dependence of yield and flow stresses, strong strain rate sensitivity, anomalous dependence of yield stress on temperature, and the breakdown of the Schmid law.

Whereas earlier studies based on empirical interatomic potentials showed the possible existence of two core variants (for review, see Reference 11), all DFT studies performed (18–24, 28,

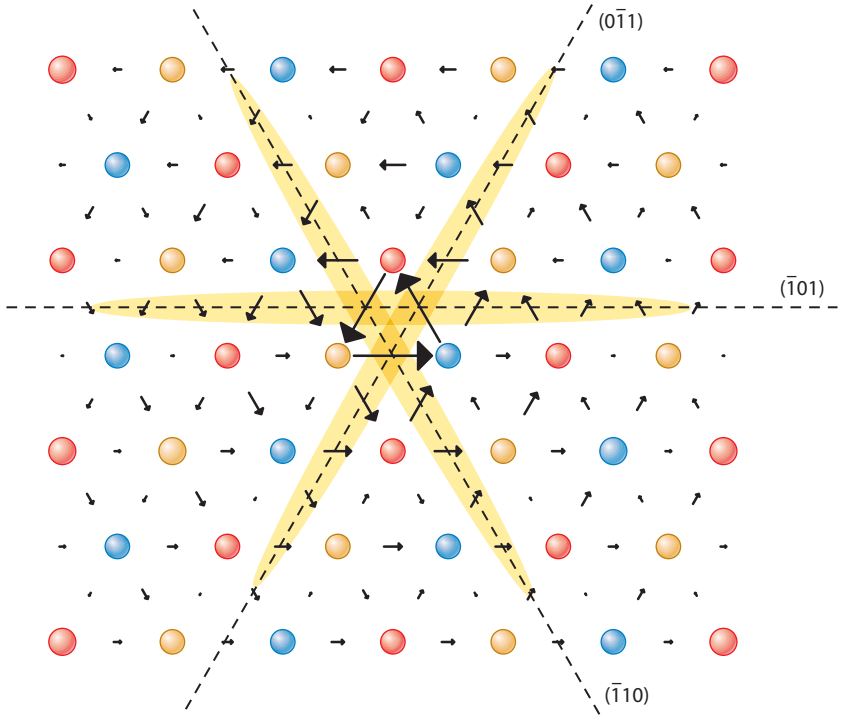

Figure 1

Equilibrium core structure of the 1/2⟨111⟩ screw dislocation in W calculated by using BOP. Colored spheres represent atoms at subsequent {111} planes; the ⟨111⟩ screw component of the relative displacement between the neighboring atoms produced by the dislocation is depicted by arrows whose length is proportional to the magnitude of these components. Adapted with permission from Reference 30.

34–36) have consistently predicted the so-called nondegenerate (also known as nonpolarized) core structure (see **Figure 1**) as the equilibrium configuration of the 1/2⟨111⟩ screw dislocation. The nondegenerate core structure was also obtained in all simulations by using semiempirical electronic structure models such as tight binding (TB), BOP, and GPT (16, 29–31, 33, 34, 37). As this result is independent of the computational methodology and boundary conditions used, the nondegenerate core structure is now broadly considered to be the generic equilibrium configuration of the 1/2⟨111⟩ screw dislocation in all pure bcc transition metals.

However, the presence of impurities or alloying elements may induce structural changes of the core. Indeed, several recent DFT calculations (23, 24, 35) have shown that alloying of W with Ta or Re leads to a transition from the nondegenerate to the degenerate core, depending on the concentration of the alloying element. In addition, as is discussed in more detail below, an application of external stresses can also significantly alter the dislocation core structure and consequently its properties.

For detailed quantitative studies of dislocation properties, realistic boundary conditions represent a crucial ingredient to obtain meaningful results. As most DFT studies employ periodic boundary conditions, dislocations are typically simulated in the form of a periodic arrangement of dipoles or quadrupoles. Because dislocations exert long-range elastic fields, it is necessary to make sure that the dislocation-dislocation interactions in small DFT supercells do not give rise to

spurious artifacts. The interaction between periodic images results in a conditional convergence of the long-range elastic fields (38, 39). These effects need to be properly taken into account when the periodic dislocation configurations are constructed (40). In addition to the long-range elastic fields, it is also necessary in small periodic supercells to correct for short-range core fields to avoid errors in the computed dislocation core energies (41–43). To overcome the limit of small supercell sizes and periodic arrangements of dislocations, Green's function flexible boundary conditions (19, 34) have been used to study isolated screw dislocations, which, however, require a nontrivial matching between the atomistic and elastic regions. All these complexities associated with simulations of dislocations by using DFT methods do not have to be considered (or are at least much less severe) for the approximate electronic structure methods (e.g., TB, BOP, GPT) that can simulate large atomic ensembles containing widely spaced or individual dislocations.

Peierls Stress, Barrier, and Potential

The goal of atomistic studies is to examine not only the intrinsic properties of dislocations at equilibrium but also especially how the dislocations respond to externally applied loads. In general, when a dislocation moves under applied stress, its core undergoes changes that are the origin of an intrinsic lattice friction. This friction is periodic with the period of the crystal. The applied stress needed to overcome this friction at 0 K is termed the Peierls stress, and the corresponding periodic energy barrier is termed the Peierls barrier. Atomistic studies employing classical interatomic potentials (for review, see, e.g., Reference 11) have revealed that the glide of the $1/2\langle 111\rangle$ screw dislocations in bcc metals is significantly affected by stress components other than those parallel to the slip direction. These so-called non-Schmid stresses do not exert any glide force on the dislocation but can change both the Peierls stress and the glide plane by altering the dislocation core structure. Direct manifestations of these atomic-scale phenomena are experimentally observed twinning-antitwinning and tension-compression asymmetries (2). To describe these effects, it is necessary to identify all components of the stress tensor that influence the motion of an individual screw dislocation and subsequently to quantify their effects on the magnitude of the Peierls stress.

The glide of the $1/2\langle 111\rangle$ screw dislocation is not confined to a single slip plane but can take place on different planes of the $\langle 111\rangle$ zone. This peculiar glide behavior is again a consequence of the nonplanar core structure and of the geometry of the bcc lattice. A complete description of the screw dislocation behavior therefore requires knowledge of the whole 2D potential energy surface—the Peierls potential—as a function of the dislocation position in the $\{111\}$ plane. Crucial to the explanation of non-Schmid effects is that this energy landscape is not stationary; rather, its magnitude and shape depend on the applied stress as a result of stress-induced transformations of the dislocation core.

Obtaining the Peierls stress and barriers from DFT calculations is complicated because of the finite size effects and strong dislocation-dislocation interactions. Ventelon and colleagues (25, 26, 40) carried out several systematic studies of the Peierls barriers in various bcc transition metals. They not only investigated transitions between the equilibrium dislocation positions (so-called easy core configurations) but also considered other dislocation configurations located at high-symmetry positions (so-called hard and split core configurations) that were expected to correspond to energy extrema (maxima or saddle points) of the Peierls potential. The main finding of these and related (22, 27) DFT studies is the existence of a smooth minimum energy path with a single energy maximum (the Peierls barrier) as the dislocation translates between the neighboring equilibrium positions on the $\{110\}$ plane. However, the nature of the saddle point (transition state) configuration and the overall topology of the Peierls potential seem to depend on the particular electronic and magnetic configuration of the transition metal (see **Figure 2**).

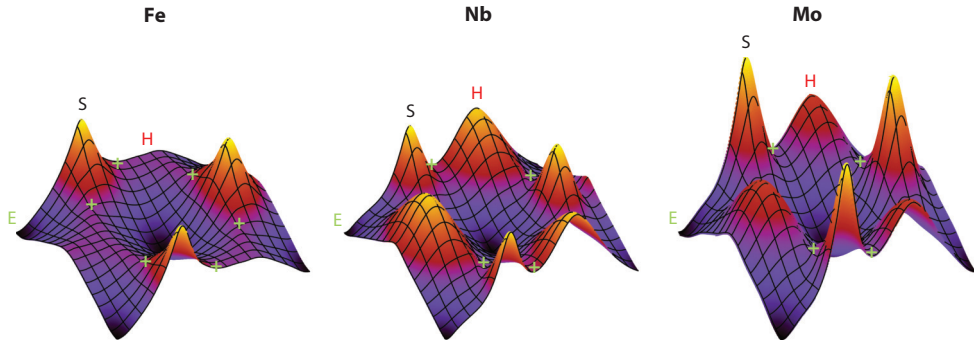

Figure 2

2D Peierls potentials for Fe, Nb, and Mo calculated by using DFT. Letters E, S, and H correspond to the easy, split, and hard core configurations, respectively; the plus symbols mark the positions of the saddle points. Adapted with permission from Reference 26.

To estimate the Peierls stress from the maximum slope of the Peierls potential along the minimum energy path, it is necessary to accurately identify the corresponding dislocation trajectory in the {111} plane during the transition. Several methods have been proposed to trace the screw dislocation either by matching the atomic positions with the anisotropic elastic displacement field (25, 44) or by using a constrained nudged elastic band method (45). Unfortunately, due to numerical inaccuracies, the error in the evaluated Peierls stresses from DFT calculations is relatively large (approximately 20%), and in some cases the minimum energy profile is not sufficiently smooth to carry out the differentiation with respect to dislocation position (26). Another limitation of the DFT calculations is that the Peierls barriers correspond only to zero-stress situations so that they cannot provide information about the stress dependences of the Peierls potential and their relation to the non-Schmid effects (44). In addition, rather large variations (of up to 40%) of the calculated barrier heights can be obtained through the use of DFT methodologies with different choices of pseudopotentials, exchange-correlation functionals, and basis sets (46, 47). Hence, it is still necessary to carefully test the convergence and the reliability of the results, especially for the saddle point configurations.

The main advantage of the semiempirical electronic structure schemes (TB, BOP, GPT) over the full quantum mechanical methods is their ability to simulate large computational blocks with flexible boundary conditions to study dislocation behavior under arbitrary external loads. During the last decade, a number of simulation studies using the BOP models (29, 30, 48–50) confirmed that structural changes of the screw dislocation core due to local stress have a profound influence on both the dislocation mobility (the Peierls stress) and the activated slip system (48, 49, 51, 52). The simulations showed that only four stress components of the full stress tensor affect the glide of the $1/2\langle 111\rangle$ screw dislocation. Two of these components are shear stresses parallel to the slip direction resolved in two different planes of the $\langle 111\rangle$ zone, whereas the other two are shear stresses perpendicular to the slip direction. The former two are necessary to explain the twinning-antitwinning asymmetry of the CRSS observed in almost all bcc metals. The latter two components cause changes of the dislocation core structure that are responsible for variations not only in the CRSS but also in the slip plane on which the dislocation moves. Koester et al. (53) recently proposed that the hydrostatic components of the stress tensor may also need to be taken into account to explain fully the non-Schmid behavior of the screw dislocation. However, the apparent influence of the hydrostatic stresses appears to be a manifestation of the effects caused by the shear stresses perpendicular to the slip direction (54).

Overall, the BOP studies showed that the detailed response of the core structure to the applied stress and thus the orientation dependencies of the yield stress as well as the slip geometry may vary significantly from one bcc metal to another. Because the BOP models are derived from quantum mechanical principles, they are more likely to provide more reliable predictions than did the empirical interatomic potentials, which were used extensively in the past. Indeed, the magnetic BOP for Fe correctly predicts not only the equilibrium dislocation properties but also the Peierls barrier in excellent quantitative agreement with DFT calculations and experimental estimates. However, due to their semiempirical nature, BOP models have limitations, and their predictions need to be validated carefully against DFT calculations and experiments.

An analytical yield criterion for the nonassociated flow in Mo, W, and Fe has been constructed from BOP studies (48, 51, 52). It closely reproduces the atomistic data not only for the glide on the primary slip system but also for slip on other planes. Theoretical predictions of this yield criterion regarding operative slip systems for uniaxial loadings in bcc single crystals agreed well with available experimental observations and provide guidance for the dislocation dynamics simulation techniques described below.

The motion of the $1/2\langle 111\rangle$ screw dislocations at finite temperatures occurs via formation and propagations of thermally activated pairs of kinks. These processes were directly investigated by molecular dynamics simulations (55–57). However, due to the limited timescale of molecular dynamics studies, the calculations had to be carried out at strain rates several orders of magnitude higher than those in typical deformation experiments. Results of such dynamics simulations are therefore valuable from a qualitative rather than a quantitative point of view. Alternative ways have been pursued by describing the thermally activated dislocation motion using mesoscopic dislocation line tension models parameterized from results of static atomistic calculations (45, 58, 59). The key quantity in these models is a stress-dependent activation enthalpy that governs the rate of dislocation motion. Because the activation enthalpy is obtained by integrating over the Peierls potential, knowledge of the dependence of the Peierls potential (or barrier) on the applied stress tensor is essential for a correct description of the thermally activated dislocation motion. Apart from studies of screw dislocations, atomistic simulations have consistently shown that the mobility of edge and mixed dislocations are significantly higher than that of the screws (60–62).

In addition to properties of individual dislocations, atomistic simulations can also provide valuable information about mutual interactions between dislocations (63, 64) as well as about interactions between dislocations and other lattice defects such as vacancies (65), interstitials, and grain boundaries (66, 67). All these interactions can lead to the pinning of dislocations, thereby decreasing their mobility. However, such interactions can also facilitate the formation of kinks on screw dislocations, thus enhancing their mobility.

MOTION OF INDIVIDUAL DISLOCATIONS

The starting point for the simulation of dislocation ensembles by a DDD approach is a model for the equation of motion for individual dislocations. As pointed out in the introduction, the motion of screw dislocations in bcc metals is thermally activated and is affected by the local stress state. There is general agreement that the kink-pair model (13, 14) can describe the thermally activated screw dislocation mobility. The model requires an activation enthalpy, which can be obtained in various ways. In the pioneering work of Tang et al. (68), the glide of individual screw dislocations in Ta was parameterized on the basis of macroscopic measurement of an effective activation enthalpy for a macroscopic stress state within a phenomenological Kocks model approach (68–70). The model has been refined to lead to a reasonable limit of zero velocity at zero stress (71) by including kink-pair nucleation in forward and backward directions with respect to the applied stress in the glide

plane of the dislocation. The DDD simulations (68) reproduced the overall experimental behavior and recovered the activation enthalpy implemented in the mobility law. This result led the authors to conclude that individual screw dislocation properties are experimentally measurable. The role of dislocation interactions was found not to be important for the studied single slip orientation (68). However, the framework did not include non-Schmid effects and, taking the global stress state for the parameterization, implicitly disregarded local stress variations due to dislocation interactions.

Chaussidon et al. (57, 72) proposed, for α-iron, a first approach to include stresses other than the resolved shear stress on the glide plane and to incorporate atomistic information on twinning-antitwinning asymmetry on screw dislocation glide. As before, the activation enthalpy was fitted to experiments, but the cross-slip rules between the allowed {110} slip planes were adapted to distinguish between screw dislocation glide in twinning and antitwinning directions as found by atomistic simulations. This approach allowed for the simulation of the dislocation structures forming at different temperatures in Fe laths (72).

In an alternative approach, Gröger, Vitek, and colleagues (50, 52, 58) based the constitutive law for the glide of screw dislocations directly on atomistic results. This approach has now been further extended (73) and is explained below because it offers the ability to directly base DDD simulations on fundamental atomistic dislocation properties. The formulation is based on the classical model of Dorn & Rajnak (14) regarding the elementary process of kink-pair formation and the propagation of the kinks along the screw dislocation.

Experimental observations of dislocation microstructures in bcc metals at low temperatures show almost exclusively long screw dislocations (2, 74). At higher temperatures, this predominance of screw dislocations is reduced, and a more fcc-like dislocation network is observed. This microstructural difference has a direct consequence on the internal stress distribution in dislocation networks in bcc metals. Above the athermal temperature, the local stresses on different segments of the dislocations control the dislocations' motion. The dislocation microstructure may then safely be assumed to be close to equilibrium, meaning that the local curvature is equilibrating the shear stress acting locally. This high-temperature case is not dealt with here.

A completely different situation is obtained at low temperature. In this case, it is assumed that all nucleated kinks move rapidly along the screw dislocation and that all nucleated kinks on one screw dislocation therefore contribute to dislocation motion. Remote effects, such as kink-pair nucleation occurring somewhere along the dislocation, contribute to the local mobility, and local velocity depends linearly on the length L of the screw dislocation. The effective velocity v of a screw dislocation is then given by

$$v = \frac{b a_0 L}{l_c^2} \upsilon_D e^{-\frac{\Delta H(\boldsymbol{\sigma})}{k_B T}}, \qquad 1.$$

where b is the length of Burgers vector, a_0 the elementary kink height in the glide plane of the screw dislocation, l_c the critical length for the nucleation of the kink pair, υ_D the Debye frequency, $\Delta H(\boldsymbol{\sigma})$ the activation enthalpy, $\boldsymbol{\sigma}$ the stress tensor acting along the dislocation line, k_B the Boltzmann constant, and T the temperature. The kink-pair model for dislocation motion is described in detail in References 15 and 75. The critical quantity in Equation 1 is the stress-dependent activation enthalpy, which can be determined directly from atomistic calculations, as detailed in the subsection "Peierls Stress, Barrier, and Potential."

Because recent experiments (76, 77) and atomistic results show that the elementary planes of slip of screw dislocations are {110} planes only (31, 49, 50, 52, 58), effective slip on other (irrational) planes is regarded as composed of elementary steps on {110} planes (73). An important extension to the initial work of Gröger and colleagues (50, 52, 58) is to consider all {110} planes as possible glide planes for a given screw dislocation. Gröger and colleagues (50, 52, 58) found that the stress

dependency of the activation enthalpy can be parameterized by only three parameters: (*a*) the angle χ between the maximum resolved shear stress plane (MRSSP) and the primary glide plane, (*b*) the shear stress τ in the MRSSP, and (*c*) the ratio η of the shear stress in a plane perpendicular to the MRSSP and the shear stress τ. If one takes these three parameters into account, the total velocity $\boldsymbol{v}_{\mathrm{tot}}$ of a screw dislocation is given by the sum of the velocities v_{gp} on the three possible {110} glide planes (gp) and reads

$$\boldsymbol{v}_{\mathrm{tot}} = \sum_{\mathrm{gp} \in \text{ allowed}\{110\} \text{ planes}} v_{\mathrm{gp}} \boldsymbol{s}_{\mathrm{gp}}. \qquad 2.$$

The direction $\boldsymbol{s}_{\mathrm{gp}}$ is perpendicular to the screw dislocation line direction within the glide plane gp, pointing in the direction of kink nucleation (forward jumps). The velocities v_{gp} are then controlled by the three activation enthalpies $\Delta H_{\mathrm{gp}}(\chi, \eta, \tau)$ via Equation 1. The velocity $\boldsymbol{v}_{\mathrm{tot}}$ gives the effective slip direction and is perpendicular to the screw dislocation line. In DDD codes, the effective glide direction can be realized by glide on the two most active {110} planes by using a probability scheme to switch between the {110} systems (57, 72, 73).

At low temperature, the local stress state along a dislocation line and nonlocal effects on dislocation mobility become increasingly important. A screw dislocation is influenced by the stress state along its entire length because the kink-pair nucleation rate varies locally according to Equation 1. The local kink-pair nucleation probability is integrated over the entire screw dislocation by splitting the dislocation line into N segments with length l_i, where l_i is the length of the ith segment and is chosen short enough to capture local stress variations. For glide on a specific glide plane gp, the screw dislocation velocity v_{gp} is then given by

$$v_{\mathrm{gp}} = \sum_{n=1}^{N} v_n = \frac{b a_0}{l_{\mathrm{c}}^2} \upsilon_{\mathrm{D}} \sum_{n=1}^{N} l_n e^{-\frac{\Delta H_{\mathrm{gp}}(\chi,\eta,\tau)}{k_{\mathrm{B}} T}}, \qquad 3.$$

where the summation goes over the N segments of the screw dislocation section. This summation over all N segments implies that all generated kinks contribute to the forward motion of the screw dislocation. Cross-slip and the splitting of screw dislocations onto different glide planes due to locally differing stresses are described in detail in References 73 and 78. Effects of (interstitial) impurities or point defects on kink-pair nucleation and dislocation mobility have not yet been addressed for discrete dislocation modeling.

Within the proposed multiscale framework, we now address some open questions in the understanding of the deformation behavior of bcc metals at low temperature. The first issue is the very high Peierls stresses predicted by atomistic studies exceeding the experimental values by a factor of 3–5. There are in principle two questions to be raised. (*a*) Is the Peierls stress of an individual screw dislocation experimentally measurable? (*b*) Is the comparison done for the same loading conditions? The latter point is especially important due to the role of non-Schmid stresses in screw dislocation glide.

To address the first question, collective dislocation effects in a dislocation pileup were considered (79) to explain the discrepancy between experiment and simulation. The stress on the first dislocation was, of course, effectively higher than the applied stress needed for its glide. The formation of the pileup configuration, however, remained somewhat unclear, as all screw dislocations within the pileup would also have to somehow overcome the Peierls stress.

The second question concerns the role of loading conditions. Because of the stress dependence of the activation enthalpy, the Peierls stress is also expected to depend on the loading conditions. This aspect has been addressed in References 15, 50, and 73. As an example, for W, one finds a reduction of the Peierls stress for uniaxial loading of approximately 25% compared with pure shear loading. Nevertheless, there is still a significant discrepancy between the experimental and

atomistic values. This discrepancy may be further reduced by taking into account dislocation-dislocation interactions and the role of other materials defects in the activation enthalpy.

Recent TEM observations of the glide of individual dislocations in pure Fe at room temperature confirm that screw dislocations glide smoothly with a velocity proportional to their length. Slip is confined to {110} planes only (76), and a transition to jerky motion is found for temperatures below $T = 250$ K (77). A hypothetical mechanism based on a metastable glissile core configuration of screw dislocations has been suggested (77) to explain this transition but has not yet been found in atomistic simulations. Thus, the transition to jerky motion remains an interesting subject for further investigations.

In 1956, quantum effects were mentioned by Mott (80) for low-temperature creep and by Seeger (13) to explain internal friction data at low temperature. The quantum mechanical effect would limit the localization of the screw dislocation within the Peierls valley and would therefore lead to a lower Peierls stress. Recently, Proville et al. (81) calculated, within a quantum transition state theory, the kink-pair formation enthalpy and found a decrease due to the quantization of the crystal vibrational modes. The resulting Peierls stress is closer to the experimental values and strongly depends on non-Schmid effects (82). Gilbert et al. (83) included both stress and temperature in the formulation of a Peierls free energy $G_P(T, \sigma)$ and showed that the critical stress is lowered by, e.g., approximately 60% at $T = 100$ K. Together with nonlocal effects due to dislocation interactions, the temperature- and stress-dependent Peierls free energy promises to capture a good part of the remaining discrepancy between atomistic single-dislocation properties and experiments at intermediate temperatures.

DISLOCATION INTERACTIONS

Dislocation interactions play a fundamental role in the hardening behavior of materials and the formation of patterns (84). Slip system interaction parameters for crystal plasticity models have been determined by dislocation dynamics simulations, e.g., for α-Fe in the athermal regime (85). The work has been extended to derive a crystal plasticity law for low- and high-temperature deformation, including particle-strengthening mechanisms also covering the transition between both regimes (86).

On a more microscopic level, the role of dislocation interactions is well illustrated with the example of simulating small-scale testing of a W micropillar. Within the DDD framework, a small-scale testing sample with a square cross section of side length 0.5 μm and a height of 1.5 μm can be completely described in terms of boundary conditions and loading geometry. The big unknown—compared with experiments—is usually the initial dislocation microstructure. The simplest choice for dislocation microstructure is to start with a few initially straight dislocation segments mimicking Frank-Read sources. Uniaxial tension or compression simulations at 300 K with dislocation mobility as described above were performed under displacement control to allow for stress relaxation within the sample (78, 87).

The tension-compression asymmetry is clearly visible in **Figure 3*a*** for the initial yield point in the chosen [$\bar{1}$49] loading direction. Initial yielding at very low stress is governed by the operation of the sources that form a structure consisting of pure screw dislocations, piercing through the sample surfaces. Usually no dislocation reactions occur within the dislocation structure. When significant plastic yielding begins, the initially straight screw dislocations start gliding, and a stress drop is observed. This initial yielding is accompanied by a steep increase in dislocation density, as displayed in **Figure 3*b***. Dislocation motion in the dislocation network is then aided by short-range interactions that lead to local stress maxima and increased mobility of screw dislocations due to non-Schmid stresses. These local hot spots trigger the glide of the entire long screw dislocation,

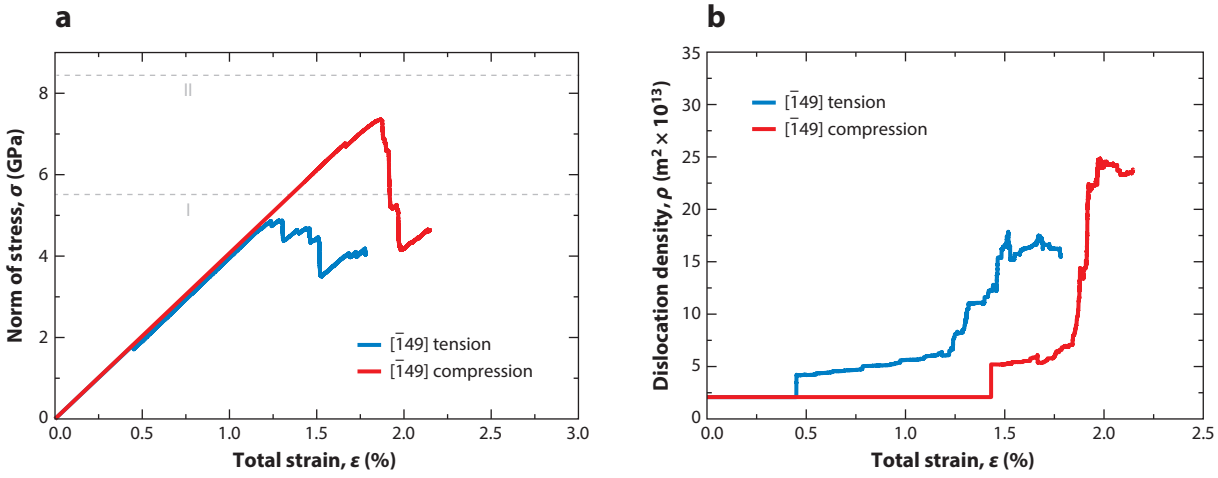

Figure 3

(*a*) Stress-versus-strain curve for pillar deformation along the [1̄49] direction in tension (*blue line*) and compression (*red line*); the gray dashed lines (I) and (II) are reference lines for the critical stress from atomistic calculations on the glide plane with maximal Schmid factor. (*b*) The corresponding dislocation density evolution. Adapted with permission from Reference 78.

which may even move other hitherto immobile screw dislocations. The observed stress drop is approximately 1 GPa in tension and more than 3 GPa in compression, in which non-Schmid effects are more relevant. The stress-strain curves of the DDD simulations shown in **Figure 3*a*** closely resemble experimental results for small W pillars (87).

ANOMALOUS SLIP AND SMALL-SCALE TESTING

The occurrence of plastic slip on planes with a much lower resolved shear stress than that of the primary slip systems is termed anomalous slip and is common in many high-purity bcc materials at low temperature (2, 15). It was first observed in Nb (4) but is absent in α-Fe (88). Non-Schmid effects and surface effects are commonly assumed to be possible origins of anomalous slip. Surface effects are assumed to trigger anomalous slip because kinks can nucleate at surfaces more easily due to image forces (89). Recent molecular dynamics and DDD simulations (90) indicated that this mechanism may be important. However, the extremely high stresses that were needed for the very small specimens leave doubts about the generality of these findings. An alternative explanation may be coplanar double slip (91), by which a network of screw dislocations is assumed to be generated in the anomalous plane and local interactions of the screw dislocations are proposed to greatly enhance their mobility (91). Atomistic studies have indeed shown a somewhat enhanced mobility of the screw dislocations due to network crossing (63), but DDD simulations (78) indicate that mobility is enhanced only at very short distances and only for attractively interacting dislocations.

Advances in in situ observation methods during microtesting, such as Laue microdiffraction (92, 93), now allow for the study of slip activity, particularly anomalous slip activity, with an unprecedented richness of detail. Compression tests on W micropillars (87) show clear slip traces from primary and secondary slip systems as well as those from anomalous slip. Anomalous slip occurred consecutively and alternately with slip on primary and secondary systems (87). This finding points to the key role of dislocation-dislocation interactions as the origin for anomalous slip in W. Through the use of the above DDD simulation setup for W (73), cross-kinks were identified

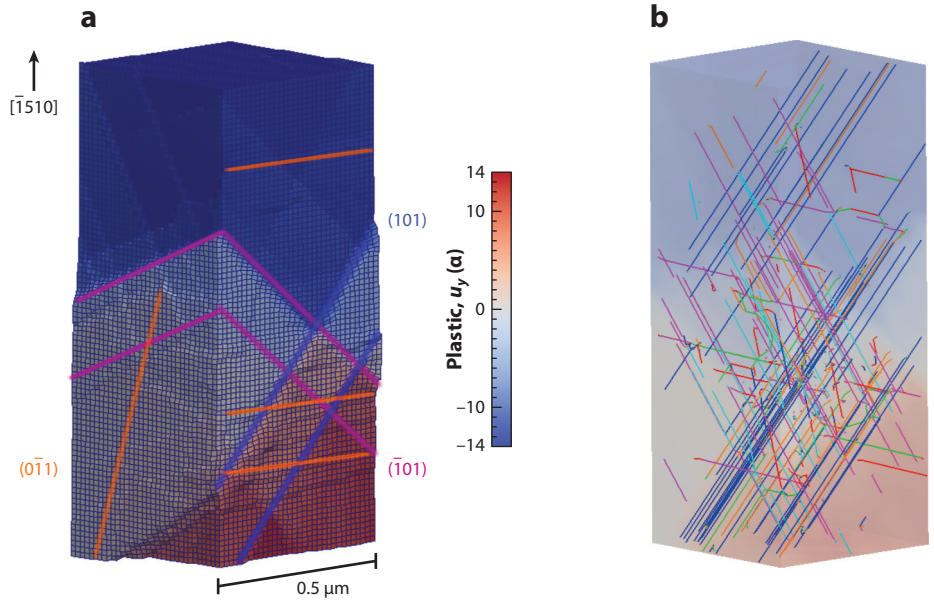

Figure 4

(*a*) Deformed pillar loaded under compression along the [$\bar{1}$510] direction, colored according to the *y*-component of the total plastic displacement at a total plastic strain of 0.8%, in units of lattice constant. The plastic deformation is scaled by a factor of 15 and is added to the undeformed geometry. The slip traces of the primary ($\bar{1}$01), conjugate (101), and anomalous (0$\bar{1}$1) systems are marked by purple, blue, and orange lines, respectively. The traces of the anomalous (0$\bar{1}$1) slip are best visible on the right side parallel to the orange lines, whereas only faint traces are visible on the left side due to the orientation of the Burgers vector. (*b*) The corresponding dislocation microstructure dominated by long, straight screw dislocations.

as the origin of the anomalous slip in this case (87). Cross-kinks are formed by interactions of dislocations on the primary glide planes and can generate highly mobile mixed dislocation segments that cross the entire specimen and produce clear slip traces on the surface (see **Figure 4**).

This example demonstrates that non-Schmid effects together with the nonlocal nature of screw dislocation mobility may lead to unexpected new mobile dislocation arrangements, which are relevant for explaining the deformation process in bcc metals. To describe these phenomena, a continuum plasticity formulation has to explicitly account for the dislocation populations, and the probability of occurrence of such events has to be systematically studied.

More generally, deformation experiments on small-scale samples with at least one dimension in the range of micrometers have revealed size effects in the flow stress (see References 94 and 95 for review). For bcc metals, the behavior is different in the low-temperature and high-temperature regimes. Below the athermal temperature, the size effect in bcc metals is weak (96, 97), whereas above the athermal temperature, it is almost as pronounced as in fcc metals. This effect is independent of a single-slip or multislip crystal orientation, which led to the interpretation that interactions between slip systems do not control the size effect (96, 97). This interpretation is further supported by the observation that prestraining has little effect on mechanical behavior (98). However, the relative orientation of the most active slip systems with respect to the sample surfaces is an important factor of influence. If the specimen geometry is chosen such that either long or short screw dislocations control the plastic flow, the latter geometry shows systematically lower flow stresses, which again indicates that interaction of screw dislocations with the specimen

surface may be important. In summary, one can certainly conclude that modern small-scale testing, together with in situ observation techniques, promises to reveal many important aspects about plastic deformation of bcc metals that may in the future be systematically analyzed with atomistically informed DDD simulations.

CONTINUUM DISLOCATION THEORY

Classical models of continuum plasticity in bcc metals are built upon considerations of only single screw dislocations and directly relate macroscopic properties of bcc metals to dislocation core effects. Basic models typically ignore the collective behavior and effects resulting from interactions between dislocations. Hardening has in the recent past been incorporated into extensions of such models by phenomenological hardening laws (86, 99–103). The original model for strain hardening that is unanimously used in these crystal plasticity descriptions dates back to the work of Kocks (70) and was originally developed for fcc crystals. Despite subsequent refinements, these models remain completely phenomenological due to the underlying premise that local dislocation multiplication is governed by the plastic strain rate. Macroscopically, this concept is useful, but on scales below the characteristic length scale of dislocation structures, it contradicts the physics of plastic deformation. Within microstructural scales, high-dislocation-density regions develop in areas of low dislocation activity, whereas regions of high plastic slip may become depleted of dislocations. These observations directly contradict the paradigm implicitly contained in Kocks-type models. Evidently, modeling plasticity on these scales requires the consideration of dislocation fluxes and the kinematics of moving dislocations. This requirement is evident for small-scale materials behavior that may be tackled by DDD simulations but also holds for continuum plasticity formulations that aim at including microstructural information. The latter requires a continuum theory of dislocation dynamics able to describe dislocation line length changes and changes of dislocation character.

So far, most of the progress in developing continuum dislocation dynamics (CDD) descriptions by derivation of averaged theories of dislocations has been made in the context of fcc materials. The progress has now reached a level at which transferring these methods to bcc crystals has become feasible. With the peculiar properties of screw dislocations in bcc metals and the resulting uneven dislocation density distributions, such developments are still at an infant stage. In this section, we summarize the progress in averaging evolving dislocation systems and give a perspective on applying these methods to bcc materials.

Kröner (104) originally suggested the derivation of continuum theories of dislocations by using averaging methods from statistical mechanics. A statistical continuum theory of dislocations was worked out more than 30 years later for simplified, quasi-2D systems of straight, parallel edge dislocations (105). This theory is based on densities of positive ρ_+ and negative ρ_- edge dislocations. When dislocation sources are neglected, the evolution equations for these densities are conservation laws, $\partial_t \rho_\pm = -\mathrm{div}(v\rho_\pm \boldsymbol{m}_\pm)$, where v denotes the dislocation velocity and $\boldsymbol{m}_\pm$ the normalized slip direction. The achievement here was the derivation of the average dislocation velocity such that it accounts for collective effects of dislocations. The average dislocation velocity contains not only the resolved shear stress but two further stress contributions that account for short-range interactions: a Taylor-type flow stress and a so-called back stress that depends on the gradient of the geometrically necessary dislocations. The statistical mechanics theory was the only continuum model that was able to reproduce the strain and dislocation density distribution observed in the discrete dislocation simulations (106, 107). However, the advantage of the statistical mechanics–based theory over phenomenological theories stemmed from the right reflection of dislocation kinematics rather than from a superior strain gradient formulation.

Reflecting the kinematics of the system in density variables is trivial for the case of straight, parallel edge dislocations in which the conservation law takes the form of a divergence. The generalization of the divergence equation to a corresponding averaged conservation law for systems of curved dislocations has turned out to be markedly more difficult (108). Although a conservation law for curved dislocation lines is in principle known (109), this curl-type equation is restricted to continuum theories with a high spatial resolution; in this case, all dislocations are geometrically necessary, as in DDD simulations. Averaged descriptions for curved dislocation were proposed on the basis of distinguishing between positive and negative densities of edge and screw dislocations (110–112). Although these approaches consider dislocation fluxes, they suffer from cumbersome rules for (or ignorance of) dislocation line length changes and line direction changes during the motion of dislocations. A straightforward generalization of the signed densities in the quasi-2D theory is to introduce a higher-dimensional dislocation density function that depends on dislocation line direction (113, 114). Nevertheless, higher-dimensional descriptions succeeded only after the introduction of an additional density variable to ensure the connectivity of dislocation lines, which is essentially a measure for the density of curvature of the dislocation lines (115).

Of course, such a higher-dimensional theory (115) is of limited practical use (116). However, it is possible to derive, from the higher-dimensional theory, a kinematically consistent CDD theory (117, 118) for curved dislocations, which is (per slip system) based simply on the total dislocation density ρ, a net dislocation vector $\boldsymbol{\kappa}$, and a scalar variable q containing average information on the dislocation curvature. Therefore, such a theory does not require more variables for the characterization of the dislocation structure in an averaging volume than do the edge-screw models mentioned above.

The so-called curvature density q is a conserved quantity containing information on the total number of dislocations. This simple CDD theory requires the assumption that the dislocation velocity is independent of the dislocation character, and this theory is hence not suited for bcc metals. Also, the density of screw dislocations strongly exceeds the density of edge or mixed dislocations in bcc metals, and therefore a description based on a single total dislocation density variable seems not suitable for bcc metals at low temperature. In fact, the total dislocation density and the net dislocation vector are only the first two terms of an expansion of the higher-dimensional dislocation density into a series of symmetric alignment tensors of increasing order (119). The total dislocation density is the scalar or zeroth-order tensor, and the net dislocation vector is the first-order tensor. The next element is the recently introduced symmetric second-order dislocation alignment tensor $\boldsymbol{\rho}^{(2)}$ (119). The physical content of this tensor is that it assigns a total dislocation vector $\boldsymbol{\rho}(\boldsymbol{\xi})$ to an oriented surface element with unit normal $\boldsymbol{\xi}$ through $\boldsymbol{\rho}(\boldsymbol{\xi}) = \boldsymbol{\xi}\cdot\boldsymbol{\rho}^{(2)}$. The tensor may be pictured as a sum of the unit tangent vectors of dislocations piercing an oriented surface element. In a coordinate system aligned with screw and edge directions (and slip plane normal), the in-plane diagonal components of $\boldsymbol{\rho}^{(2)}$ correspond to the total density of screw and edge dislocations. The off-diagonal element $\rho_{12} = \rho_{21}$, by contrast, cannot be interpreted as a dislocation density and may take negative values. Evidently, the second-order alignment tensor is closely related to the above-mentioned edge-screw models, but the decisive difference is that the screw and edge directions do not play a special role, and total densities of any mixed type of direction $\boldsymbol{l}$ may be obtained as $\rho_{ll} = \rho_{ij} l_i l_j$.

An evolution equation for the second-order alignment tensor was given in Reference 119, but only for isotropic dislocation mobility. A version that may take into account anisotropic dislocation velocities as needed for bcc metals was recently developed (120). If we assume that the velocity of a dislocation with a line direction inclined by an angle α to the Burgers vector is given by

$$v(\alpha) = v_s \cos^2 \alpha + v_e \sin^2 \alpha, \qquad 4.$$

where v_s denotes the velocity of a screw dislocation and v_e the velocity of an edge dislocation, the directional dependence of the velocity assumes an elliptic directional dependence. This dependency may also be expressed by a second-order tensor

$$\boldsymbol{v}^{(2)} = \begin{pmatrix} v_{11} & v_{12} \\ v_{21} & v_{22} \end{pmatrix} = \begin{pmatrix} v_s & 0 \\ 0 & v_e \end{pmatrix}. \quad 5.$$

With this elliptic velocity distribution, the evolution of the total dislocation density, the dislocation density vector, and the second-order dislocation density tensor takes the form (120)

$$\partial_t \rho = \partial_i (v_{kl} \varepsilon_{ij} \rho_{klj}) + v_{kl} \varepsilon_{km} Q_{mn}, \quad 6.$$

$$\partial_t \kappa_i = -\varepsilon_{ij} \partial_j (v_{kl} \rho^{kl}), \quad 7.$$

$$\partial_t \rho_{ij} = -\varepsilon_{im} \partial_m (v_{kl} \rho_{klj}) + v_{kl} Q_{ijkl} - \rho_{klmin} \varepsilon_{jn} \partial_m v_{kl} - v_{kl} (Q_{kjli} + Q_{ljki}), \quad 8.$$

where $\varepsilon_{ij} = n^k \varepsilon_{ikj}$ is the tensor that tilts vectors in the slip plane by 90°, i.e., the cross-product with the slip plane normal $\boldsymbol{n}$ (ε_{ikj} denotes the totally antisymmetric Levi-Civita symbol). In these evolution equations, the symmetric dislocation density tensors (ρ_{ijk}, ρ_{ijklm}) and curvature tensors (Q_{ij}, Q_{ijkl}) appear to order five and four, respectively. In fact, these evolution equations are part of an infinite hierarchy of evolution equations of alignment tensors of increasing order. To be useful, this hierarchy has to be terminated at low order. The lowest order for which this termination seems meaningful in the bcc case is second order. All tensors of higher order need to then be obtained from closure assumptions. The most simple closure assumptions take the expression known for single dislocations to define simple product expressions for higher-order tensors in terms of lower-order ones (120). More sophisticated closure assumptions may be obtained from a maximum entropy approach, as suggested in Reference 121.

We note that Equation 6 is redundant, as it is derived by taking the trace of Equation 8, and that Equation 7 is in principle well known, as it expresses the definition of the dislocation density tensor as the curl of the plastic distortion tensor. What makes Equation 8 unique and markedly different from classical edge-screw approaches is that it contains the right kinematics of evolving curved dislocations. In Equation 8, the first term is a curl-type dislocation flux expression; the second term is a product of dislocation velocity and curvature, which describes line length increase and virtual rotations of dislocation segments; the third term (which is traceless) describes segment rotations due to spatial gradients of the dislocation velocity; and the fourth term (which is also traceless) accounts for segment reorientation due to the directionally dependent velocity, which tends to rotate curved dislocation segments. Notably, the second term $v_{kl} Q_{ijkl}$ contains the production of screw dislocation density from the motion of edge dislocations and vice versa. This production obviously depends on the curvature of the dislocations because long, straight screw segments do not produce edge dislocations, whereas (expectedly) curved edge segments increase the screw density. The consideration of different curvatures for edge and screw segments requires at least a second-order curvature tensor similar to the second-order alignment tensor. Therefore, Equations 6–8 need to be complemented with suitable evolution equations for dislocation curvature variables.

In this article, we discuss only the kinematic aspects of the anisotropic CDD theory, omitting the modeling of the dislocation velocity and its dependence on the surrounding dislocation state. As long as collective dislocation effects are of secondary importance, CDD may use essentially the same velocity laws as does DDD. In general, however, the velocity tensor in the CDD formulation rather stands for an average velocity of dislocations of a given type. For the quasi-2D case of straight, parallel edge dislocations, a velocity law was derived by using pair correlation functions,

which turned out to be short ranged. It may safely be assumed that similar stress contributions will also be of importance in 3D systems. Because dislocations will generally be curved, an additional line tension contribution has been suggested (117). However, there is little hope to be able to apply the same strategy as in the quasi-2D theory, for which pair correlations of dislocations have been obtained from a huge number of relaxed dislocation configurations. Pair correlation functions in bcc metals (Mo) have been obtained from 3D discrete dislocation simulations (122–124). But the analyzed pair correlations were obtained from high-strain-rate simulations and show dependency on initial dislocation structure and loading configuration. Consequently, such pair correlations have not been turned into a constitutive model for a kinetic theory of dislocations.

OUTLOOK

Building up a physically based multiscale simulation model for bcc materials involves challenges at all involved scales. At the atomic scale, reliable approaches based on quantum mechanical principles have provided important quantitative information about the energetics of dislocations at 0 K, but the analysis in terms of the activation enthalpies and free energies that are necessary for description of dislocation behavior at finite temperatures is still largely unexplored. In addition, studies of mutual interactions between dislocations as well as between dislocations and other lattice defects and impurities certainly deserve further attention. Recent atomistic calculations as well as in situ TEM experiments have consistently shown that the elementary glide of the $1/2\langle 111\rangle$ screw dislocations occurs exclusively on the $\{110\}$ planes. No evidence of core transformations at elevated temperatures, which was proposed to explain the transition from $\{110\}$ to $\{112\}$ glide in some bcc metals (125), has been found. Instead, both the lattice resistance and the net glide plane (126) seem to be controlled primarily by core transformation due to the applied stress, including the nonglide (non-Schmid) components of the stress tensor.

At the mesoscopic level, the DDD models rely on accurate mobility laws. Recent attempts to derive the mobility laws for screw dislocations based on atomistic approaches have proven to be successful. First studies of multidislocation problems during deformation of pillars have revealed interesting new phenomena and may help to explain hitherto seemingly contradicting experimental observations. Further DDD investigations of multidislocation behavior need to aim at direct quantitative comparison of the computed mechanical properties, e.g., flow stresses, with small-scale experiments. To reach this, it is necessary to parameterize the dislocation mobilities for various bcc metals and to consider effects of vacancies, self-interstitials, impurities, and eventually grain boundaries to address the plasticity of polycrystalline materials. The emergent new phenomena in multidislocation simulations occur as a consequence of the local action of stresses between dislocations and their effect on the screw dislocation mobility. Direct dislocation-dislocation core interactions may introduce new and unexplored effects (127). These phenomena, however, should probably be investigated simultaneously through the use of large-scale atomistic simulations and TEM studies.

At the macroscopic level, CDD provides a new perspective for deriving mesoscopic crystal plasticity laws for bcc metals entirely on the basis of dislocation density variables. However, CDD still bears many open questions and challenges, most obviously regarding the to-be-derived constitutive equations for the dislocation velocity. As discussed above, there is little hope that direct averaging of 3D discrete dislocation results may be employed in the same way as it has been in the quasi-2D theory. A more promising starting point for a generalization to 3D systems may be the variational formulation recently presented in References 128 and 129 for the quasi-2D case or the additional consideration of specific dislocation configurations like dipoles in the formulation of the averaging procedures (130). Even then, further corrections may be required

to take into account additional microstructural elements that lead to pileups and to strong local lattice curvature (131). A 3D generalization of dipole interactions is available from the multipole expansion of dislocation interactions suggested in References 132 and 133. In that theory, a local distribution of dislocation lines is expanded into geometric multipole moments in finite averaging volumes. It seems promising to connect the local multipole expansion into alignment tensors with the geometrical multipole moments to obtain averaged descriptions of dislocation interactions.

Aside from the question of constitutive modeling, the kinematic evolution equations of CDD represent a new type of conservation law for tensorial representations of line densities. These are strongly coupled systems of partial differential equations containing flux and source terms. Preliminary studies show that the consideration of a Taylor-type hardening term in the velocity seems to make the equations inherently unstable, leading to the emergence of inhomogeneous dislocation structures. This result may be expected because this Taylor hardening triggers a feedback loop in which high-dislocation-density regions lead to low dislocation velocities such that dislocations get trapped in these regions and the density increases further (134). Although this feature may be desirable for a physical theory of dislocation plasticity, in which dislocation structures are ubiquitously observed, it is a challenge for numerical simulations.

DISCLOSURE STATEMENT

The authors are not aware of any affiliations, memberships, funding, or financial holdings that might be perceived as affecting the objectivity of this review.

ACKNOWLEDGMENTS

This work was funded by the German Research Foundation (DFG) under projects Gu 367/30 and HO 4227/3-1 as well as under the research group FOR 1650, and by the European Commission under contract NMP.2010.2.5-1.263335 (MultiHy).

LITERATURE CITED

1. Taylor GI, Elam CF. 1926. The distortion of iron crystals. *Proc. R. Soc. A* 112(761):337–61
2. Christian JW. 1983. Some surprising features of the plastic deformation of body-centered cubic metals and alloys. *Metall. Trans. A* 14(7):1237–56
3. Schmid E, Boas W. 1935. *Kristallplastizität unter besonderer Berücksichtigung der Metalle*. Berlin: Julius Springer
4. Duesbery MS, Foxall RA. 1969. A detailed study of the deformation of high purity niobium single crystals. *Philos. Mag.* 20(166):719–51
5. Bolton CJ, Taylor G. 1972. Anomalous slip in high-purity niobium single crystals deformed at 77°K in tension. *Philos. Mag.* 26(6):1359–76
6. Matsui H, Kimura H. 1976. Anomalous {110} slip in high-purity molybdenum single crystals and its comparison with that in V(a) metals. *Mater. Sci. Eng.* 24(2):247–56
7. Duesbery MS, Vitek V. 1998. Plastic anisotropy in b.c.c. transition metals. *Acta Mater.* 46(5):1481–92
8. Hsiung LL. 2010. On the mechanism of anomalous slip in bcc metals. *Mater. Sci. Eng. A* 528(1):329–37
9. Vítek V, Perrin RC, Bowen DK. 1970. The core structure of 1/2⟨111⟩ screw dislocations in b.c.c. crystals. *Philos. Mag.* 21(173):1049–73
10. Vitek V. 1992. Structure of dislocation cores in metallic materials and its impact on their plastic behaviour. *Prog. Mater. Sci.* 36:1–27
11. Vitek V, Paidar V. 2008. Non-planar dislocation cores: a ubiquitous phenomenon affecting mechanical properties of crystalline materials. *Dislocations Solids* 14:441

12. Cai W, Bulatov VV, Chang J, Li J, Yip S. 2004. Dislocation core effects on mobility. In *Dislocations in Solids*, ed. FRN Nabarro, JP Hirth, pp. 1–80. Amsterdam: Elsevier
13. Seeger A. 1956. On the theory of the low-temperature internal friction peak observed in metals. *Philos. Mag.* 1(7):651–62
14. Dorn E, Rajnak S. 1964. Nucleation of kink pairs and the Peierls' mechanism of plastic deformation. *Trans. AIME* 230:1052–64
15. Kubin LP. 2013. *Dislocations, Mesoscale Simulations and Plastic Flow*. Oxford, UK: Oxford Univ. Press
16. Moriarty JA, Vitek V, Bulatov VV, Yip S. 2002. Atomistic simulations of dislocations and defects. *J. Comput. Mater. Des.* 9:99–132
17. Pettifor DG. 1995. *Bonding and Structure of Molecules and Solids*. Oxford, UK: Oxford Univ. Press
18. Ismail-Beigi S, Arias T. 2000. Ab initio study of screw dislocations in Mo and Ta: a new picture of plasticity in bcc transition metals. *Phys. Rev. Lett.* 84(7):1499–502
19. Woodward C, Rao S. 2002. Flexible ab initio boundary conditions: simulating isolated dislocations in bcc Mo and Ta. *Phys. Rev. Lett.* 88(21):216402
20. Trinkle DR, Woodward C. 2005. The chemistry of deformation: how solutes soften pure metals. *Science* 310(5754):1665–67
21. Shimizu F, Ogata S, Kimizuka H, Kano T, Li J, Kaburaki H. 2007. First-principles calculation on screw dislocation core properties in bcc molybdenum. *J. Earth Simulator* 7(March):17–21
22. Itakura M, Kaburaki H, Yamaguchi M. 2012. First-principles study on the mobility of screw dislocations in bcc iron. *Acta Mater.* 60(9):3698–710
23. Romaner L, Ambrosch-Draxl C, Pippan R. 2010. The effect of rhenium on the dislocation core structure in tungsten. *Phys. Rev. Lett.* 104:195503
24. Samolyuk GD, Osetsky YN, Stoller RE. 2013. The influence of transition metal solutes on the dislocation core structure and values of the Peierls stress and barrier in tungsten. *J. Phys. Condens. Matter.* 25(2):025403
25. Ventelon L, Willaime F, Clouet E, Rodney D. 2013. Ab initio investigation of the Peierls potential of screw dislocations in bcc Fe and W. *Acta Mater.* 61(11):3973–85
26. Dezerald L, Ventelon L, Clouet E, Denoual C, Rodney D, Willaime F. 2014. Ab initio modeling of the two-dimensional energy landscape of screw dislocations in bcc transition metals. *Phys. Rev. B* 89(2):024104
27. Weinberger C, Tucker G, Foiles S. 2013. Peierls potential of screw dislocations in bcc transition metals: predictions from density functional theory. *Phys. Rev. B* 87(5):054114
28. Frederiksen SL, Jacobsen KW. 2003. Density functional theory studies of screw dislocation core structures in bcc metals. *Philos. Mag.* 83(3):365–75
29. Mrovec M, Nguyen-Manh D, Pettifor D, Vitek V. 2004. Bond-order potential for molybdenum: application to dislocation behavior. *Phys. Rev. B* 69(9):094115
30. Mrovec M, Gröger R, Bailey AG, Nguyen-Manh D, Elsässer C, Vitek V. 2007. Bond-order potential for simulations of extended defects in tungsten. *Phys. Rev. B* 75(10):104119
31. Mrovec M, Nguyen-Manh D, Elsässer C, Gumbsch P. 2011. Magnetic bond-order potential for iron. *Phys. Rev. Lett.* 106(24):246402
32. Lin Y, Mrovec M, Vitek V. 2014. A new method for development of bond-order potentials for transition bcc metals. *Model. Simul. Mater. Sci. Eng.* 22:034002
33. Moriarty JA, Benedicta LX, Gloslia JN, Hooda RQ, Orlikowskia DA, et al. 2006. Robust quantum-based interatomic potentials for multiscale modeling in transition metals. *J. Mater. Res.* 21(3):563–73
34. Rao SI, Woodward C. 2001. Atomistic simulations of (a/2)⟨111⟩ screw dislocations in bcc Mo using a modified generalized pseudopotential theory potential. *Philos. Mag. A* 81(5):1317–27
35. Li H, Wurster S, Motz C, Romaner L, Ambrosch-Draxl C, Pippan R. 2012. Dislocation-core symmetry and slip planes in tungsten alloys: ab initio calculations and microcantilever bending experiments. *Acta Mater.* 60(2):748–58
36. Ventelon L, Willaime F. 2010. Generalized stacking-faults and screw-dislocation core-structure in bcc iron: a comparison between ab initio calculations and empirical potentials. *Philos. Mag.* 90(7–8):1063–74
37. Mrovec M, Elsässer C, Gumbsch P. 2010. Atomistic simulations of lattice defects in tungsten. *Int. J. Refract. Met. Hard Mater.* 28(6):698–702

38. Li J, Wang C-Z, Chang J-P, Cai W, Bulatov V, et al. 2004. Core energy and Peierls stress of a screw dislocation in bcc molybdenum: a periodic-cell tight-binding study. *Phys. Rev. B* 70(10):104113
39. Cai W, Bulatov VV, Chang J, Li J, Yip S. 2003. Periodic image effects in dislocation modelling. *Philos. Mag.* 83(5):539–67
40. Ventelon L, Willaime F. 2008. Core structure and Peierls potential of screw dislocations in α-Fe from first principles: cluster versus dipole approaches. *J. Comput. Mater. Des.* 14(Suppl. 1):85–94
41. Clouet E, Ventelon L, Willaime F. 2009. Dislocation core energies and core fields from first principles. *Phys. Rev. Lett.* 102(5):055502
42. Clouet E. 2011. Dislocation core field. I. Modeling in anisotropic linear elasticity theory. *Phys. Rev. B* 84(22):224111
43. Clouet E, Ventelon L, Willaime F. 2011. Dislocation core field. II. Screw dislocation in iron. *Phys. Rev. B* 84(22):224107
44. Rodney D, Proville L. 2009. Stress-dependent Peierls potential: influence on kink-pair activation. *Phys. Rev. B* 79(9):094108
45. Gröger R, Vitek V. 2012. Constrained nudged elastic band calculation of the Peierls barrier with atomic relaxations. *Model. Simul. Mater. Sci. Eng.* 20(3):035019
46. Ventelon L, Willaime F, Clouet E, Rodney D. 2013. Ab initio investigation of the Peierls potential of screw dislocations in bcc Fe and W. *Acta Mater.* 61(11):3973–85
47. Weinberger C, Tucker G, Foiles S. 2013. Peierls potential of screw dislocations in bcc transition metals: predictions from density functional theory. *Phys. Rev. B* 87(5):054114
48. Vitek V, Mrovec M, Gröger R, Bassani JL, Racherla V, Yin L. 2004. Effects of non-glide stresses on the plastic flow of single and polycrystals of molybdenum. *Mater. Sci. Eng. A* 387–389(1–2):138–42
49. Chen ZM, Mrovec M, Gumbsch P. 2013. Atomistic aspects of 1/2⟨111⟩ screw dislocation behavior in α-iron and the derivation of microscopic yield criterion. *Model. Simul. Mater. Sci. Eng.* 21(5):055023
50. Gröger R, Bailey AG, Vitek V. 2008. Multiscale modeling of plastic deformation of molybdenum and tungsten. I. Atomistic studies of the core structure and glide of 1/2⟨111⟩ screw dislocations at 0 K. *Acta Mater.* 56(19):5401–11
51. Vitek V, Mrovec M, Bassani JL. 2004. Influence of non-glide stresses on plastic flow: from atomistic to continuum modeling. *Mater. Sci. Eng. A* 365(1–2):31–37
52. Gröger R, Racherla V, Bassani JL, Vitek V. 2008. Multiscale modeling of plastic deformation of molybdenum and tungsten. II. Yield criterion for single crystals based on atomistic studies of glide of 1/2⟨111⟩ screw dislocations. *Acta Mater.* 56(19):5412–25
53. Koester A, Ma A, Hartmaier A. 2012. Atomistically informed crystal plasticity model for body-centered cubic iron. *Acta Mater.* 60(9):3894–901
54. Gröger R. 2014. Which stresses affect the glide of screw dislocations in bcc metals? *Philos. Mag.* 94(18):2021–30
55. Domain C, Monnet G. 2005. Simulation of screw dislocation motion in iron by molecular dynamics simulations. *Phys. Rev. Lett.* 95(21):215506
56. Marian J, Cai W, Bulatov VV. 2004. Dynamic transitions from smooth to rough to twinning in dislocation motion. *Nat. Mater.* 3(3):158–63
57. Chaussidon J, Fivel M, Rodney D. 2006. The glide of screw dislocations in bcc Fe: atomistic static and dynamic simulations. *Acta Mater.* 54(13):3407–16
58. Gröger R, Vitek V. 2008. Multiscale modeling of plastic deformation of molybdenum and tungsten. III. Effects of temperature and plastic strain rate. *Acta Mater.* 56(19):5426–39
59. Proville L, Ventelon L, Rodney D. 2013. Prediction of the kink-pair formation enthalpy on screw dislocations in α-iron by a line tension model parametrized on empirical potentials and first-principles calculations. *Phys. Rev. B* 87(14):144106
60. Monnet G, Terentyev D. 2009. Structure and mobility of the 1/2 ⟨111⟩ {112} edge dislocation in bcc iron studied by molecular dynamics. *Acta Mater.* 57(5):1416–26
61. Kang K, Bulatov VV, Cai W. 2012. Singular orientations and faceted motion of dislocations in body-centered cubic crystals. *PNAS* 109(38):15174–78
62. Weinberger CR. 2010. Dislocation drag at the nanoscale. *Acta Mater.* 58(19):6535–41

63. Bulatov V, Cai W. 2002. Nodal effects in dislocation mobility. *Phys. Rev. Lett.* 89(11):115501
64. Bulatov VV, Hsiung LL, Tang M, Arsenlis A, Bartelt MC, et al. 2006. Dislocation multi-junctions and strain hardening. *Nature* 440(7088):1174–78
65. Chen ZM, Mrovec M, Gumbsch P. 2011. Dislocation–vacancy interactions in tungsten. *Model. Simul. Mater. Sci. Eng.* 19(7):074002
66. Cheng Y, Mrovec M, Gumbsch P. 2008. Atomistic simulations of interactions between the 1/2⟨111⟩ edge dislocation and symmetric tilt grain boundaries in tungsten. *Philos. Mag.* 88(4):547–60
67. Mrovec M, Elsässer C, Gumbsch P. 2009. Interactions between lattice dislocations and twin boundaries in tungsten: a comparative atomistic simulation study. *Philos. Mag.* 89(34–36):3179–94
68. Tang M, Kubin LP, Canova GR. 1998. Dislocation mobility and the mechanical response of b.c.c. single crystals: a mesoscopic approach. *Acta Mater.* 46(9):3221–35
69. Kocks UF, Argon AS, Ashby MF. 1975. *Thermodynamics and Kinetics of Slip* (Progress in Materials Science, Vol. 19). New York: Pergamon
70. Kocks UF. 1976. Laws for work-hardening and low-temperature creep. *J. Eng. Mater. Technol.* 98(1):76–85
71. Naamane S, Monnet G, Devincre B. 2010. Low temperature deformation in iron studied with dislocation dynamics simulations. *Int. J. Plast.* 26(1):84–92
72. Chaussidon J, Robertson C, Rodney D, Fivel M. 2008. Dislocation dynamics simulations of plasticity in Fe laths at low temperature. *Acta Mater.* 56(19):5466–76
73. Srivastava K, Gröger R, Weygand D, Gumbsch P. 2013. Dislocation motion in tungsten: atomistic input to discrete dislocation simulations. *Int. J. Plast.* 47:126–42
74. Louchet F, Kubin LP. 1975. Dislocation substructures in the anomalous slip plane of single crystal niobium strained at 50 K. *Acta Metall.* 23(1):17–21
75. Argon AS. 2008. *Strengthening Mechanisms in Crystal Plasticity*. Oxford, UK: Oxford Univ. Press
76. Caillard D. 2010. Kinetics of dislocations in pure Fe. I. In situ straining experiments at room temperature. *Acta Mater.* 58(9):3493–503
77. Caillard D. 2010. Kinetics of dislocations in pure Fe. II. In situ straining experiments at low temperature. *Acta Mater.* 58(9):3504–15
78. Srivastava K. 2014. *Atomistically-informed discrete dislocation dynamics modeling of plastic flow in body-centered cubic metals*. PhD Thesis, Karlsruhe Inst. Technol.
79. Gröger R, Vitek V. 2007. Explanation of the discrepancy between the measured and atomistically calculated yield stresses in body-centered cubic metals. *Philos. Mag. Lett.* 87(2):113–20
80. Mott NF. 1956. Creep in metal crystals at very low temperatures. *Philos. Mag.* 1(6):568–72
81. Proville L, Rodney D, Marinica M-C. 2012. Quantum effect on thermally activated glide of dislocations. *Nat. Mater.* 11(10):845–49
82. Barvinschi B, Proville L, Rodney D. 2014. Quantum Peierls stress of straight and kinked dislocations and effect of non-glide stresses. *Model. Simul. Mater. Sci. Eng.* 22(2):25006
83. Gilbert MR, Schuck P, Sadigh B, Marian J. 2013. Free energy generalization of the Peierls potential in iron. *Phys. Rev. Lett.* 111(9):095502
84. LeSar R. 2014. Simulations of dislocation structure and response. *Annu. Rev. Condens. Matter Phys.* 5(1):375–407
85. Queyreau S, Monnet G, Devincre B. 2009. Slip systems interactions in α-iron determined by dislocation dynamics simulations. *Int. J. Plast.* 25(2):361–77
86. Monnet G, Vincent L, Devincre B. 2013. Dislocation-dynamics based crystal plasticity law for the low- and high-temperature deformation regimes of bcc crystal. *Acta Mater.* 61(16):6178–90
87. Marichal C, Srivastava K, Weygand D, Van Petegem S, Grolimund D, et al. 2014. Origin of anomalous slip in tungsten. *Phys. Rev. Lett.* 113(2):025501
88. Aono Y, Kuramoto E, Kitajima K. 1981. Plastic deformation of high-purity iron single crystals. *Rep. Res. Inst. Appl. Mech.* 29:127–93
89. Matsui H, Kimura H. 1973. A mechanism of the "unexpected {110} slip" observed in bcc metals deformed at low temperatures. *Scr. Metall.* 7(9):905–13
90. Weinberger CR, Cai W. 2008. Surface-controlled dislocation multiplication in metal micropillars. *PNAS* 105(38):14304–7

91. Matsui H, Kimura H. 1975. Anomalous {110} slip and the role of co-planar double slip in bcc metals. *Scr. Metall.* 9(9):971–78
92. Barabash RI, Ice GE, Walker FJ. 2003. Quantitative microdiffraction from deformed crystals with unpaired dislocations and dislocation walls. *J. Appl. Phys.* 93(3):1457
93. Van Swygenhoven H, Van Petegem S. 2010. The use of Laue microdiffraction to study small-scale plasticity. *JOM* 62(12):36–43
94. Uchic MD, Shade PA, Dimiduk DM. 2009. Plasticity of micrometer-scale single crystals in compression. *Annu. Rev. Mater. Res.* 39(1):361–86
95. Kraft O, Gruber PA, Mönig R, Weygand D. 2010. Plasticity in confined dimensions. *Annu. Rev. Mater. Res.* 40(1):293–317
96. Schneider AS, Kaufmann D, Clark BG, Frick CP, Gruber PA, et al. 2009. Correlation between critical temperature and strength of small-scale bcc pillars. *Phys. Rev. Lett.* 103(10):105501
97. Schneider AS, Frick CP, Clark BG, Gruber PA, Arzt E. 2011. Influence of orientation on the size effect in bcc pillars with different critical temperatures. *Mater. Sci. Eng. A* 528(3):1540–47
98. Schneider AS, Clark BG, Frick CP, Gruber PA, Arzt E. 2010. Effect of pre-straining on the size effect in molybdenum pillars. *Philos. Mag. Lett.* 90(11):841–49
99. Peeters B, Kalidindi SR, Van Houtte P, Aernoudt E. 2000. A crystal plasticity based work-hardening/softening model for b.c.c. metals under changing strain paths. *Acta Mater.* 48(9):2123–33
100. Stainier L, Cuitiño AM, Ortiz M. 2002. A micromechanical model of hardening, rate sensitivity and thermal softening in BCC single crystals. *J. Mech. Phys. Solids* 50(7):1511–45
101. Ma A, Roters F, Raabe D. 2007. A dislocation density based constitutive law for BCC materials in crystal plasticity FEM. *Comput. Mater. Sci.* 39(1):91–95
102. Alankar A, Field DP, Raabe D. 2014. Plastic anisotropy of electro-deposited pure α-iron with sharp crystallographic $\langle 111 \rangle$ texture in normal direction: analysis by an explicitly dislocation-based crystal plasticity model. *Int. J. Plast.* 52:18–32
103. Knezevic M, Beyerlein IJ, Lovato ML, Tomé CN, Richards AW, McCabe RJ. 2014. A strain-rate and temperature dependent constitutive model for BCC metals incorporating non-Schmid effects: application to tantalum–tungsten alloys. *Int. J. Plast.* 62(0):93–104
104. Kröner E. 1969. Initial studies of a plasticity theory based upon statistical mechanics. In *Inelastic Behavior of Solids*, ed. MF Kanninen, WF Adler, AR Rosenfield, RI Jaffee, pp. 137–47. New York: McGraw-Hill
105. Groma I, Csikor FF, Zaiser M. 2003. Spatial correlations and higher-order gradient terms in a continuum description of dislocation dynamics. *Acta Mater.* 51:1271–81
106. Yefimov S, Groma I, van der Giessen E. 2004. A comparison of a statistical-mechanics based plasticity model with discrete dislocation plasticity calculations. *J. Mech. Phys. Solids* 52:279–300
107. Bittencourt E, Needleman A, Gurtin ME, van der Giessen E. 2003. A comparison of nonlocal continuum and discrete dislocation plasticity predictions. *J. Mech. Phys. Solids* 51:281–310
108. Kröner E. 2001. Benefits and shortcomings of the continuous theory of dislocations. *Int. J. Solids Struct.* 38(6–7):1115–34
109. Mura T. 1963. Continuous distribution of moving dislocations. *Philos. Mag.* 8(89):843–57
110. Arsenslis A, Parks DM, Becker R, Bulatov VV. 2004. On the evolution of crystallographic dislocation density in non-homogeneously deforming crystals. *J. Mech. Phys. Solids* 52:1213–46
111. Reuber C, Eisenlohr P, Roters F, Raabe D. 2014. Dislocation density distribution around an indent in single-crystalline nickel: comparing nonlocal crystal plasticity finite-element predictions with experiments. *Acta Mater.* 71:333–48
112. Zaiser M, Hochrainer T. 2006. Some steps towards a continuum representation of 3D dislocation systems. *Scr. Mater.* 54(5):717–21
113. Kosevich AM. 1979. Crystal dislocations and theory of elasticity. In *Dislocations in Solids*, ed. FRN Nabarro, pp. 33–142. Amsterdam: North Holland
114. El-Azab A. 2000. Statistical mechanics treatment of the evolution of dislocation distributions in single crystals. *Phys. Rev. B* 61(18):11956–66
115. Hochrainer T, Zaiser M, Gumbsch P. 2007. A three-dimensional continuum theory of dislocation systems: kinematics and mean-field formulation. *Philos. Mag. A* 87(8):1261–82

116. Sandfeld S, Hochrainer T, Zaiser M, Gumbsch P. 2010. Numerical implementation of a 3D continuum theory of dislocation dynamics and application to microbending. *Philos. Mag.* 90(27):3697–728
117. Hochrainer T, Sandfeld S, Zaiser M, Gumbsch P. 2014. Continuum dislocation dynamics: towards a physical theory of crystal plasticity. *J. Mech. Phys. Solids* 63(1):167–78
118. Ebrahimi A, Monavari M, Hochrainer T. 2014. Numerical implementation of continuum dislocation dynamics with the discontinuous-Galerkin method. *MRS Proc.* 1651; doi: 10.1557/opl.2014.26
119. Hochrainer T. 2014. Continuum dislocation dynamics based on the second order alignment tensor. *MRS Proc.* 1651; doi: 10.1557/opl.2014.53
120. Hochrainer T. 2015. Multipole expansion of continuum dislocations dynamics in terms of alignment tensors. *Philos. Mag.* In press
121. Monavari M, Zaiser M, Sandfeld S. 2014. Comparison of closure approximations for continuous dislocation dynamics. *MRS Proc.* 1651; doi: 10.1557/opl.2014.62
122. El-Azab A, Deng J, Tang M. 2007. Statistical characterization of dislocation ensembles. *Philos. Mag.* 87(8–9):1201–23
123. Deng J, El-Azab A. 2007. Dislocation pair correlations from dislocation dynamics simulations. *J. Comput. Mater. Des.* 14(1):295–307
124. Deng J, El-Azab A. 2007. Mathematical and computational modelling of correlations in dislocation dynamics. *Model. Simul. Mater. Sci. Eng.* 17(1):75010
125. Seeger A. 2004. Experimental evidence for the {110}-{112} transformation of the screw-dislocation cores in body-centred cubic metals. *Phys. Status Solid.* 201(4):R21–24
126. Weinberger CR, Boyce BL, Battaile CC. 2013. Slip planes in bcc transition metals. *Int. Mater. Rev.* 58(5):296–314
127. Srivastava K, Weygand D, Gumbsch P. 2014. Dislocation junctions as indicators of elementary slip planes in body-centered cubic metals. *J. Mater. Sci.* 49(20):7333–37
128. Groma I, Györgyi G, Ispánovity PD. 2010. Variational approach in dislocation theory. *Philos. Mag.* 90(27–28):3679–95
129. Groma I, Vandrus Z, Ispanovity DP. 2015. Scale-free phase field theory of dislocations. *Phys. Rev. Lett.* 114(1):015503
130. Dickel D, Schulz K, Schmitt S, Gumbsch P. 2014. Dipole formation and yielding in a two-dimensional continuum dislocation model. *Phys. Rev. B* 90(9):094118
131. Schulz K, Dickel D, Schmitt S, Sandfeld S, Weygand D, Gumbsch P. 2014. Analysis of dislocation pile-ups using a dislocation-based continuum theory. *Model. Simul. Mater. Sci. Eng.* 22(2):025008
132. LeSar R, Rickman JM. 2002. Multipole expansion of dislocation interactions: application to discrete dislocations. *Phys. Rev. B* 65(14):144110
133. LeSar R, Rickman JM. 2004. Incorporation of local structure in continuous dislocation theory. *Phys. Rev. B* 69(17):172105
134. Zaiser M, Sandfeld S. 2014. Scaling properties of dislocation simulations in the similitude regime. *Model. Simul. Mater. Sci. Eng.* 22:065012